Published online before print July 22, 2008
(*Radiology* 2008, 10.1148/radiol.2483071400)

Musculoskeletal Imaging

Rotator Cuff in Asymptomatic Volunteers: Contrast-enhanced US Depiction of Intratendinous and Peritendinous Vascularity[1]

Ronald S. Adler, PhD, MD, Stephen Fealy, MD, Jonas R. Rudzki, MD, Warren Kadrmas, MD, Nikhil N. Verma, MD, Andrew Pearle, MD, Stephen Lyman, PhD, and Russell F. Warren, MD

[1] From Weill Medical College of Cornell University, New York, NY (R.S.A.); Department of Radiology and Imaging, Division of Ultrasound and Body Imaging (R.S.A.), Sports Service at Department of Orthopaedics (S.F., A.P., R.F.W., W.K.), and Epidemiology and Biostatistics Division (S.L.), Hospital for Special Surgery, 535 E 70th St, New York, NY 10021; Washington Orthopaedics and Sports Medicine, Washington, DC (J.R.R.); and Midwest Orthopaedics at Rush, Chicago, Ill (N.N.V.). Received August 8, 2007; revision requested October 5; revision received January 2, 2008; accepted January 30; final version accepted March 28. Supported in part by research grants provided by Major League Baseball (grant 3135400), the Soft Tissue Research Fund of the Hospital for Special Surgery, and Philips Medical Systems. **Address correspondence to** R.S.A. (e-mail: *adlerr@hss.edu*).

ABSTRACT

Purpose: To test the hypothesis that regional variations in supraspinatus tendon vascularity exist and can be imaged and quantified in asymptomatic individuals by using contrast material–enhanced ultrasonography (US).

Materials and Methods: After institutional review board approval and informed consent were obtained, 31 volunteers aged 22–65 years (mean age, 41.5 years) underwent lipid microsphere contrast-enhanced shoulder US performed with an L8-4 transducer operating in contrast harmonic mode and a mechanical index of 0.07 in a HIPAA-compliant protocol. Images were obtained in the volunteers at rest and after exercise. Quantitative analysis was performed by using the time-enhancement postcontrast data derived from four regions of interest (ROIs): bursal medial, articular medial, bursal lateral, and articular lateral. Two 2-minute acquisitions were performed after each contrast material bolus. Baseline enhancement and peak enhancement for each ROI were estimated from these acquisitions. Baseline gray-scale and power Doppler US images of the supraspinatus tendon were obtained by using an L12-5 transducer. The Mann-Whitney nonparametric test was used to test for significant differences between ROIs in all volunteers.

Results: In the volunteers at rest before exercise, significant variations in regional enhancement between the articular medial zone and both the bursal medial zone ($P = .002$) and the bursal lateral zone ($P = .003$) were observed. Differences in enhancement between the articular medial and articular lateral zones approached significance. Greater differentiation ($P < .001$) was observed after exercise, with a significant increase in apparent enhancement in each ROI in all volunteers.

Conclusion: This study revealed the spatial distribution of the blood supply to the supraspinatus tendon in asymptomatic individuals. The addition of exercise to the protocol resulted in a significantly increased level of enhancement compared with that at rest and enabled more sensitive assessment of intratendinous and peritendinous vascularity.

Supplemental material: *http://radiology.rsnajnls.org/cgi/content/full/2483071400/DC1*

INTRODUCTION

Chronic rotator cuff tendinopathy and tearing have been associated with extrinsic subacromial impingement and intrinsic degenerative changes, among other factors. These other factors include both intrinsic biologic factors, such as the role of matrix metalloproteinase expression, and morphologic factors, such as tendon vascularity (1–6). The hypothesis that there is an association between rotator cuff disease and tendon vascularity is based on the results of cadaveric studies that have demonstrated a region of hypovascularity at the articular surface of the distal aspect of the supraspinatus tendon, or the so-called critical zone (7–10). The age-dependent alterations that occur in the blood supply to the rotator cuff and the role of this supply in the origin of rotator cuff disease have not been definitively established in vivo. A study involving the use of orthogonal polarization microscopy at arthroscopy revealed a significant decrease in the microcirculation adjacent to rotator cuff lesions (11).

The potential role of vascularity in the pathogenesis of rotator cuff tendinopathy requires further study, as it may have important implications for understanding the natural history of the disease and the development and application of surgical and biologic interventions. Methods currently used to image the rotator cuff in vivo include magnetic resonance (MR) and ultrasonography (US); however, methods of looking specifically at the microcirculation have been limited (12,13). Before now, to our knowledge, there was no diagnostic modality with the capability to noninvasively and reliably depict the vascular anatomy of the rotator cuff dynamically in vivo in asymptomatic individuals. This study was designed to test the hypothesis that regional variations in supraspinatus tendon vascularity exist and can be imaged and quantified with contrast material–enhanced US in asymptomatic individuals.

MATERIALS AND METHODS

Demographic Data

After institutional review board approval was obtained, 31 volunteers (13 men, 18 women; mean age, 41.5 years; age range, 22–65 years) underwent lipid microsphere (perflutren, Definity; Bristol-Meyers Squibb, North Billerica, Mass) contrast-enhanced US of a randomly selected shoulder (14,15). Sixteen volunteers were younger than 40 years, and 15 were older than 40 years. Exclusion criteria included a history of shoulder abnormality, tobacco use, or cardiovascular disease and a partial-thickness rotator cuff tear involving more than 50% of the thickness of the tendon. Informed consent for this Health Insurance Portability and Accountability Act–compliant study was obtained from all volunteers before contrast material administration. The contrast agent was obtained for off-label use with funds provided by grant support. The US examinations were performed between December 2005 and April 2006.

US Imaging

To optimally visualize the intratendinous blood flow to the supraspinatus tendon, US images were obtained at baseline, after contrast material administration with the volunteer at rest, and after contrast material administration after the volunteer had exercised. Anatomic baseline gray-scale and power Doppler images of the supraspinatus tendon were obtained by using an L12-5 phased-array linear transducer and an IU22 US scanner (Philips Medical Systems, Bothell, Wash) (Fig 1). To visualize the supraspinatus tendon, scanning was performed with the arm in internal rotation and mild hyperextension. Images were obtained in the long axis of the tendon to enable visualization of the myotendinous junction, the articular portion of the tendon, and the footprint at the greater tuberosity (13). During baseline scanning, a surgical marker was used to place marks on the skin surface to help reproduce the transducer position. The low-flow settings on the scanner were used to obtain power Doppler images to discern any baseline vascularity and to serve as a reference imaging plane for observation. All scanning examinations were performed by one sonographer (R.S.A.), who is a musculoskeletal radiologist with 19 years experience. Two additional investigators—an orthopedic fellow (J.R.R. or A.P.) and a staff orthopedic surgeon (S.F.)—were present during each examination. One of the additional investigators administered the contrast material and monitored the volunteer, while the second was present as an observer.

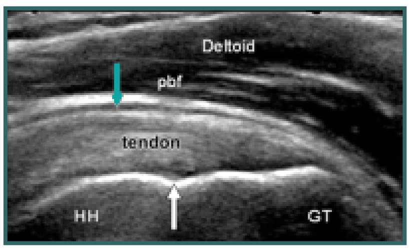

View larger version (99K):
[in this window]
[in a new window]
[Download PPT slide]

Figure 1a: **(a)** Supraspinatus tendon depicted on normal long-axis gray-scale US image in 32-year-old asymptomatic man. The tendon is echogenic with a convex margin and is inserting onto the greater tuberosity *(GT)*. Humeral head *(HH)*, peribursal fat *(pbf)*, and deltoid muscle are labeled. Peribursal fat is a thin echogenic line below the hypoechoic deltoid muscle. Green arrow points to subdeltoid bursa, which appears as a thin hypoechoic line deep to the peribursal fat. A small cortical depression (white arrow) points to the anatomic neck. **(b)** Baseline long-axis power Doppler US image of supraspinatus tendon obtained by using low-flow setting in 64-year-old asymptomatic man shows two peribursal vessels and no intratendinous vessels. Low level of background noise (color) is evident. The large vessels (far left) were persistent findings when observed in real time. The remaining tiny flecks of orange, likely representing noise, were inconsistent during real-time observation. Redder hues correspond to greater intensity of the Doppler signal. Number scale at right is in centimeters.

View larger version (87K):
[in this window]
[in a new window]
[Download PPT slide]

Figure 1b: **(a)** Supraspinatus tendon depicted on normal long-axis gray-scale US image in 32-year-old asymptomatic man. The tendon is echogenic with a convex margin and is inserting onto the greater tuberosity *(GT)*. Humeral head *(HH)*, peribursal fat *(pbf)*, and deltoid muscle are labeled. Peribursal fat is a thin echogenic line below the hypoechoic deltoid muscle. Green arrow points to subdeltoid bursa, which appears as a thin hypoechoic line deep to the peribursal fat. A small cortical depression (white arrow) points to the anatomic neck. **(b)** Baseline long-axis power Doppler US image of supraspinatus tendon obtained by using low-flow setting in 64-year-old asymptomatic man shows two peribursal vessels and no intratendinous vessels. Low level of background noise (color) is evident. The large vessels (far left) were persistent findings when observed in real time. The remaining tiny flecks of orange, likely representing noise, were inconsistent during real-time observation. Redder hues correspond to greater intensity of the Doppler signal. Number scale at right is in centimeters.

Initially, a baseline anatomic scan was obtained with the L12-5 transducer to confirm an intact rotator cuff; subsequently, a 20-gauge intravenous catheter was placed in the contralateral arm. The volunteer was then administered a 4-mL bolus of a 1:10 saline-diluted preparation of the lipid microsphere contrast material (perflutren), which was followed by a 10-mL normal saline flush. After contrast material administration, scanning was performed by using an L8-4 transducer (Philips Medical Systems) operating in contrast harmonic mode and a mechanical index of 0.07 (13). Four-minute images (two 2-minute cine loops) were obtained after each bolus and transferred to a digital video disc by using the lowest level of image compression allowed for off-line US quantification and analysis (QLAB; Philips Medical Systems) with the given scanner configuration. All images were acquired in gray scale; this permitted use of the full spatial and temporal resolution of the scanner. Image acquisition was initiated at the time of bolus injection and usually resulted in a delay of approximately 20–30 seconds before the onset of contrast enhancement.

After a 10-minute rest period, the volunteer participated in an exercise protocol for optimal depiction of the vasculature of the supraspinatus tendon. Exercise consisted of two sets of 20 repetitions of forward elevation in the plane of the scapula with a 5-lb weight. Postexercise scanning was then performed (similar to the postexercise at-rest examination) after the administration of an additional 4-mL bolus of the saline-diluted lipid microsphere preparation, which was followed by a 10-mL normal saline flush.

Image Analysis

Qualitative and quantitative image analyses were performed by examining four regions of interest (ROIs) (bursal medial, articular medial, bursal lateral, and articular lateral regions) with use of US quantification and analysis software (QLAB) (Fig 2). The sonographer (R.S.A.) placed the ROIs during off-line analysis, with the requirement that each ROI be kept within the selected anatomic region during the enhancement phase. The images were transferred as a 1280 x 1028 matrix for qualitative and quantitative analyses, with the smallest ROI estimated to contain approximately 10^4 data points. Each 2-minute acquisition included approximately 1200 time points. QLAB is a previously validated software that is used in conjunction with tumor imaging after US contrast material administration and thereby enables the delineation of time-enhancement curves within a specified ROI (16). This software does not include motion compensation functions. However, it is possible to remove selected portions of the acquired data when there is translation of the relevant anatomy outside of a selected ROI. This was the case during the early part of our study, which involved examination of the first seven volunteers and during which there was a learning curve in terms of the best way to advise the volunteers on how to adjust their respiration, limit their speaking, and secure the transducer.

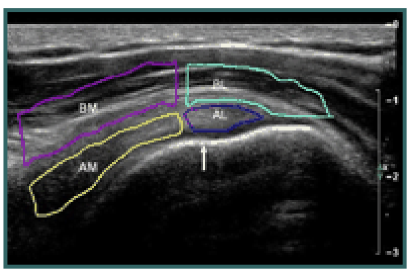

Figure 2: ROIs used for QLAB analysis in 32-year-old asymptomatic man. Bursal medial *(BM),* bursal lateral *(BL),* articular medial *(AM),* and articular lateral *(AL)* ROIs are shown. The plane of the anatomic neck (arrow) and a median line through the tendon were chosen as approximate boundaries to divide the tendon and the peribursal soft tissues into four quadrants. Number scale at right is in centimeters.

View larger version (85K):
[in this window]
[in a new window]
[Download PPT slide]

The anatomic neck served as a demarcation between the medial and lateral boundaries of the supraspinatus tendon. An approximately median line through the long axis of the tendon separated the bursal surface from the articular portion and footprint of the tendon. The bursal ROIs included the adjacent peritendinous bursal vessels. Baseline enhancement and peak enhancement were estimated for each ROI. Resultant data were assessed and expressed as values of baseline background-corrected normalized enhancement (in decibels per square millimeter) in each ROI. The obtained data were spatially averaged within each ROI to facilitate noise reduction. We also introduced a component of temporal averaging by choosing the peak values of the trend line between 1 and 3 minutes. Horizontal trend lines were drawn through the baseline and peak portions of the time-enhancement curves from which the peak and baseline values were estimated. This typically included data collected within at least 5 seconds (approximately 50 points [Fig 3]).

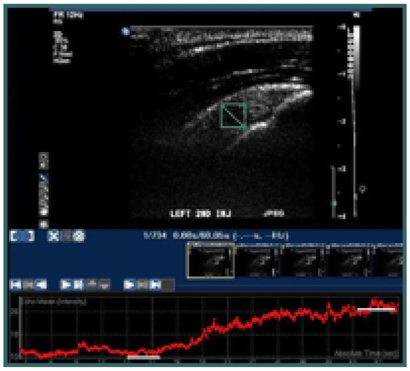

View larger version (88K):
[in this window]
[in a new window]
[Download PPT slide]

Figure 3: Example of trend behavior observed at off-line QLAB analysis of US data obtained in 32-year-old asymptomatic man. A 5-mm square ROI (green box) is placed within the articular portion of the supraspinatus tendon after exercise and contrast material administration. The data obtained within 60 seconds of a 2-minute acquisition are displayed and indicate a baseline enhancement value of approximately 10 dB, which increases to an approximate peak of 26 dB in the trend line, as delineated by the white horizontal trend lines (bottom). Yellow box depicts the first frame of the 2-minute acquisition. In this example, the background-corrected peak enhancement is estimated to be 16 dB. The horizontal trend lines cover an approximately 5-second interval, which involves approximately 50 temporal data points. The image matrix is 1280 x 1024, so the smallest ROI—an example of which is shown here—involves as many as 10^4 pixels from which the spatial average is determined. Measurements are normalized to the area within the ROI and are expressed in decibels per square millimeter. Red horizontal spectrum at bottom depicts the time-enhancement curve for the depicted ROI for the total time (abscissa) represented in this data set.

The data were subsequently assessed for patterns of anatomic enhancement to address the principal hypothesis of the current work (described earlier). As a secondary goal, we sought to determine whether any patterns based on age and sex could be discerned. Owing to the small numbers of volunteers in each age-based cohort, a detailed evaluation by decade was not feasible. However, gross patterns of separation were determined in terms of sex and age (with use of age threshold of 40 years). No volunteers had adverse reactions to the contrast agent according to blood pressure, heart rate, and pulse oximetry measurements and follow-up telephone calls 48 hours later.

Statistical Analyses

Data obtained for descriptive statistical analysis consisted of means and standard deviations for continuous variables and frequency counts and percentages for discrete variables. Inferential analysis was performed by using Kruskal-Wallis nonparametric analysis of variance with post hoc Wilcoxon signed rank nonparametric tests. Nonparametric analyses were selected owing to concerns regarding the likelihood of nonnormal data distributions. $P < .05$ was considered to indicate a significant difference. All statistical analyses were performed by using SPSS for Windows, version 13.0, software (SPSS, Chicago, Ill).

RESULTS

Imaging

Baseline power Doppler US images showed a peribursal vessel in all cases (Fig 1). In no case was intratendinous vascularity observed. At baseline contrast harmonic imaging, the deltoid muscle and supraspinatus tendon were hypoechoic, with bright linear echoes that corresponded to portions of the greater tuberosity, peribursal fat, and perimysial connective tissue of the deltoid muscle (Figs 4, 5). The residual bright reflectors presumably were due to incomplete subtraction resulting from slight misregistration or to strong stationary tissue contributions of the second-order harmonic component. Approximately 20–30 seconds after contrast material administration, the reference peribursal vessel—in addition to more extensive peribursal, muscular, and intratendinous branches—became apparent. An example of typical temporal behavior during an acquisition is shown in Figure 3. After exercise, overall enhancement within the tendon and the adjacent peribursal soft tissues increased (Figs 4, 5) *(Movies 1 and 2, http://radiology.rsnajnls.org/cgi/content/full/2483071400/DC1)*.

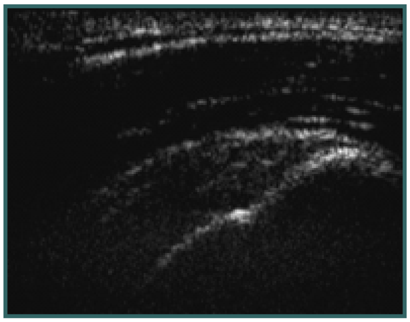

View larger version (86K):
[in this window]
[in a new window]
[Download PPT slide]

Figure 4a: Contrast harmonic images obtained in 32-year-old asymptomatic man by using pulse-inversion harmonics technique to exclude the primary frequency backscatter to the transducer. **(a)** On baseline long-axis contrast harmonic image, most of the internal echoes of the tendon are suppressed owing to use of the pulse-inversion technique. Only the most strongly reflecting surfaces, such as the cortical surface, peribursal fat, and subcutaneous fat, contribute to the observed gray-scale image. **(b)** After intravenous administration of contrast material and before cuff activation (exercise protocol), a single intratendinous peribursal vessel (arrow) is apparent. Ill-defined increased enhancement in the peribursal soft tissues is suggested, with a persistent hypoechoic area centrally at the level of the anatomic neck. **(c)** After cuff activation, there is marked enhancement of the tendon and the deltoid muscle. Note the persistent area of relative diminished flow at the articular portion of the tendon; this region corresponds to the area of low flow in **b**.

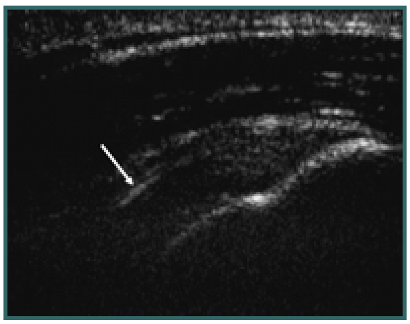

View larger version (87K):
[in this window]
[in a new window]
[Download PPT slide]

Figure 4b: Contrast harmonic images obtained in 32-year-old asymptomatic man by using pulse-inversion harmonics technique to exclude the primary frequency backscatter to the transducer. **(a)** On baseline long-axis contrast harmonic image, most of the internal echoes of the tendon are suppressed owing to use of the pulse-inversion technique. Only the most strongly reflecting surfaces, such as the cortical surface, peribursal fat, and subcutaneous fat, contribute to the observed gray-scale image. **(b)** After intravenous administration of contrast material and before cuff activation (exercise protocol), a single intratendinous peribursal vessel (arrow) is apparent. Ill-defined increased enhancement in the peribursal soft tissues is suggested, with a persistent hypoechoic area centrally at the level of the anatomic neck. **(c)** After cuff activation, there is marked enhancement of the tendon and the deltoid muscle. Note the persistent area of relative diminished flow at the articular portion of the tendon; this region corresponds to the area of low flow in **b**.

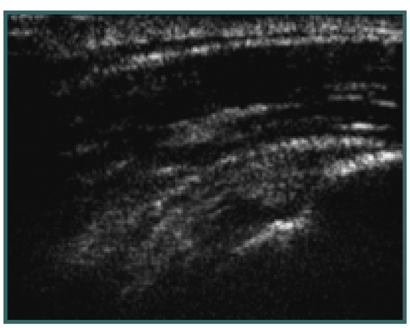

View larger version (103K):
[in this window]
[in a new window]
[Download PPT slide]

Figure 4c: Contrast harmonic images obtained in 32-year-old asymptomatic man by using pulse-inversion harmonics technique to exclude the primary frequency backscatter to the transducer. **(a)** On baseline long-axis contrast harmonic image, most of the internal echoes of the tendon are suppressed owing to use of the pulse-inversion technique. Only the most strongly reflecting surfaces, such as the cortical surface, peribursal fat, and subcutaneous fat, contribute to the observed gray-scale image. **(b)** After intravenous administration of contrast material and before cuff activation (exercise protocol), a single intratendinous peribursal vessel (arrow) is apparent. Ill-defined increased enhancement in the peribursal soft tissues is suggested, with a persistent hypoechoic area centrally at the level of the anatomic neck. **(c)** After cuff activation, there is marked enhancement of the tendon and the deltoid muscle. Note the persistent area of relative diminished flow at the articular portion of the tendon; this region corresponds to the area of low flow in **b**.

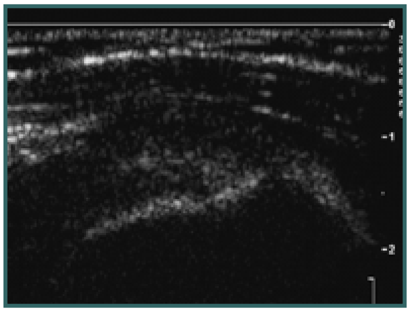

View larger version (90K):
[in this window]
[in a new window]
[Download PPT slide]

Figure 5a: Contrast harmonic long-axis images of supraspinatus tendon in 39-year-old asymptomatic woman. **(a)** Baseline image. **(b)** Image obtained after contrast material administration shows more conspicuous intratendinous vessels and peribursal enhancement. **(c)** Image obtained after exercise and contrast material administration shows marked enhancement of the tendon and the peribursal soft tissues. Time gain compensation and overall gain were fixed throughout the acquisition. Number scale at right is in centimeters.

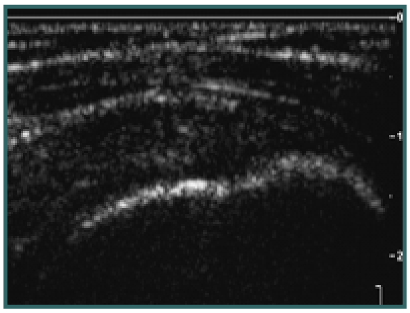

View larger version (96K):
[in this window]
[in a new window]
[Download PPT slide]

Figure 5b: Contrast harmonic long-axis images of supraspinatus tendon in 39-year-old asymptomatic woman. **(a)** Baseline image. **(b)** Image obtained after contrast material administration shows more conspicuous intratendinous vessels and peribursal enhancement. **(c)** Image obtained after exercise and contrast material administration shows marked enhancement of the tendon and the peribursal soft tissues. Time gain compensation and overall gain were fixed throughout the acquisition. Number scale at right is in centimeters.

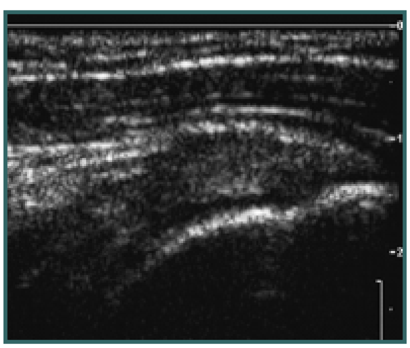

View larger version (124K):
[in this window]
[in a new window]
[Download PPT slide]

Figure 5c: Contrast harmonic long-axis images of supraspinatus tendon in 39-year-old asymptomatic woman. **(a)** Baseline image. **(b)** Image obtained after contrast material administration shows more conspicuous intratendinous vessels and peribursal enhancement. **(c)** Image obtained after exercise and contrast material administration shows marked enhancement of the tendon and the peribursal soft tissues. Time gain compensation and overall gain were fixed throughout the acquisition. Number scale at right is in centimeters.

Regional Variations in Blood Flow

Comparative analysis of blood flow differences between the four ROIs (Table) revealed a consistent region of decreased vascularity at the articular medial margin of the rotator cuff. This region had significantly less flow compared with the bursal medial ($P = .002$) and bursal lateral ($P = .003$) zones, and the difference between this region and the articular lateral zone was nearly significant ($P = .052$). After exercise, the articular medial region had significantly less flow compared with all other ROIs ($P < .002$). After exercise, a 59%–96% increase in enhancement for all regions combined ($P < .001$, Table) was observed.

View this table:	Background-corrected Peak Enhancement in Anatomic ROIs in 31 Volunteers before and after Exercise
[in this window] [in a new window]	

Our data suggest a trend toward diminished regional enhancement for each decade increase in age; there was an approximate decrease in peak enhancement of 5 dB/mm^2 per decade during the 3rd through 7th decades. However, owing to the relatively small numbers of volunteers in each decade group (five to eight individuals), these changes were not significant. When the volunteer cohort was divided into participants older than 40 years and those younger than 40 years, there was significantly increased enhancement in each anatomic ROI ($P < .04$) after exercise in the younger group. Among the 13 female and 18 male participants, there was a trend toward increased regional enhancement in the male volunteer group, although no enhancement value obtained before or after exercise was significant.

DISCUSSION

To our knowledge, this is the first study published in the radiology literature to demonstrate regional changes in vascularity in the intact rotator cuff in vivo in asymptomatic individuals. The improved sensitivity achieved by using a US contrast agent enabled the demonstration of intratendinous and peritendinous vascularity, which normally is not apparent with conventional Doppler imaging techniques (17,18).

The lipid microsphere contrast agent used (perflutren, also known as Definity) is octafluoropropane gas encased in a phospholipid shell with a mean size of 2 µm; these microspheres have a biologic half-life of 1.2 minutes (15). The lipid is metabolized in the liver, and the gas expires in the lungs. This agent has been approved by the Food and Drug Administration for use in delineating ventricular chamber borders, although it is recognized as a potential method of assessing myocardial perfusion. Noncardiac applications of this agent that have been investigated include vascular, liver, renal, and prostate examinations, with researchers in the majority of these investigations assessing it as a tumor imaging agent (19–21). Other musculoskeletal applications of US contrast material include assessment of synovial inflammation in patients with rheumatoid arthritis. The described lipid microsphere contrast agent has been used successfully in well over 50 000 patients in clinical trials, with the most common side effects being transient and including headache, flushing, chest pain, back pain, nausea, and dizziness—all of which resolve within minutes after their onset. Hypersensitivity to octafluoropropane also has been reported, although it did not occur in any of our volunteers. Several deaths during contrast-enhanced cardiac examinations in patients with severe cardiovascular disease have been reported (15,22). Whether these deaths were secondary to the contrast agent administration or were caused by the underlying disease has not been established. To our knowledge, there have been no reported deaths or serious untoward effects related to noncardiac applications of the described lipid microsphere contrast agent.

The origin of rotator cuff disease is controversial. Historically, tendon ischemia, extrinsic compression, and chronic repetitive microtrauma have been implicated as important factors in the development of rotator cuff disease. A watershed zone near the tendon footprint, referred to as the critical zone, which involves the articular portion of the cuff, is considered to be highly susceptible to the development of tendon degeneration and tearing. Although there have been anatomic study results suggesting the presence of such a hypovascular zone, noninvasive methods to assess tendon vascularity in vivo have been lacking (7–11).

The results of some investigations (23–28) have suggested that several other factors potentially contribute to the development of rotator cuff disease. Findings in exercise-based animal model studies indicate that repetitive mechanical loading of tendons may result in inflammation and degenerative change through both mechanical damage and biochemical mediators. Altered expression of degradative enzymes (metalloproteinases 1 and 3) and increased production of inflammatory mediators in response to stretching or loading in vitro are reported in the literature on fibroblast and tendon mechanobiology. Despite these developments in our understanding of the factors that may lead to intrinsic degenerative tendinopathy, the importance of considering the vascular contribution to this process remains clear (23–28). In the current study, we observed diminished vascularity of the articular portion of the supraspinatus tendon, in keeping with the concept of a critical zone. Second, vascular recruitment after an appropriate exercise regimen resulted in increased enhancement and thereby increased the effective dynamic range in which to determine differences in vascularity.

There were several limitations to this study. Slight variations in transducer positioning, as well as respiratory variation—albeit of low amplitude—could have resulted in concomitant variations in the trend behavior that manifested as small changes in amplitude. Likewise, ROIs were drawn to approximate the peribursal and tendon boundaries, although the ROIs were the same for any given 2-minute acquisition. Spatial and temporal averaging helped to circumvent the variations but did not entirely eliminate them. It was also possible to remove selected portions of the acquired data when there was translation of the relevant anatomy outside the ROI. This was the case during the early phase of the study, during which there was a learning curve in terms of how best to instruct the volunteers on how to adjust their respiration, limit their speaking, and secure the transducer. Likewise, while using the pulse-inversion technique in contrast harmonic imaging does not entirely eliminate the stationary echoes, obtaining a baseline image was useful for subtracting the contribution of the stationary reflectors. Our choice of contrast material dose, while not a limitation per se, was based largely on the minimal dose and mechanical index that yielded visually acceptable images. Better choices of dose and bolus techniques may help to optimize image acquisitions and the subsequent data analysis.

All US examinations involved imaging of a single area of the supraspinatus tendon seen on the long axis. Use of the long-axis view, however, enables simultaneous imaging of the articular and distal portions of the tendon. This made it possible to assess the peribursal, articular, and distal distributions of enhancement. Second, it is technically easier to ensure a fixed transducer position on the long axis. In the axial plane, slight changes in transducer tilt can result in visualization of the proximal or distal cuff and therefore potentially confound the results. Ideally, three-dimensional or volumetric acquisition would be the most robust method to obtain vascularity data. We believe that this may become possible in the future as two-dimensional flat-transducer arrays become readily available.

Our volunteer sample size enabled us to identify significant findings and differences at nonparametric Mann-Whitney testing; however, we believe the significance of our data would have been greater with a larger volunteer cohort. Our results suggest a possible dependence of regional enhancement degree on age, as well as possible sex-specific differences. Our study population was not large enough for us to make definitive statements with respect to either of these findings. Demonstrating an age- or sex-based dependence was not a specific goal of this work, although it would be useful to pursue these investigations in the future. It is conjectured that age probably has a role in the diminished vascularity in the critical zone and further predisposes the rotator cuff to degeneration and tearing (6).

The data were acquired and analyzed by a single highly experienced musculoskeletal sonographer. Therefore, although we believe that our intersubject analyses of the data were consistent, the lack of blinding and the absence of an additional radiologist to analyze the data may have introduced bias. In addition, the use of off-line quantitative assessment software such as that applied in this study, compared with the use of subjective image analysis, in which multiple observers are beneficial, may reduce the effect of using a single radiologist. Finally, the findings of this study are based on the assertion that peak enhancement is a function of both capillary density and regional flow.

In conclusion, we found contrast-enhanced US to be a method of displaying and quantifying regional variations in tendon vascularity within the rotator cuff of asymptomatic individuals; the potential dynamic range over which such measurements can be made improves after a standardized exercise protocol, which we hypothesize is a function of vascular recruitment. The potential applications of the described lipid microsphere enhancement technique are numerous and include determination of age-related changes in tendon vascularity, changes in vascularity in a tendinosis model, and response to physical therapy and assessment of bone tendon healing after repair.

ADVANCES IN KNOWLEDGE

- Contrast-enhanced US of the supraspinatus tendon revealed significantly lower flow ($P < .002$) in the articular medial portion of the tendon after exercise.
- There was greater differentiation after exercise, with a significant increase (59%–96%) in apparent enhancement for all regions of interest in all patients ($P < .001$).

IMPLICATIONS FOR PATIENT CARE

- TOP
- ABSTRACT
- INTRODUCTION
- MATERIALS AND METHODS
- RESULTS
- DISCUSSION
- ADVANCES IN KNOWLEDGE
- IMPLICATIONS FOR PATIENT CARE
- References

- Contrast-enhanced US of the supraspinatus tendon can be used to understand the role of vascularity in the development of rotator cuff disease.
- Contrast-enhanced US of the supraspinatus tendon could be used to measure alterations in blood flow during therapy and after tendon repair.

ACKNOWLEDGMENTS

The authors thank Ms Alana Burns, who provided organizational assistance throughout this project. The ultrasound division of Philips Medical Systems provided the QLAB software, contrast harmonics capability, and technical support to perform the contrast-enhanced US examinations.

FOOTNOTES

Abbreviations: ROI = region of interest

Author contributions: Guarantors of integrity of entire study, R.S.A., J.R.R., S.L.; study concepts/study design or data acquisition or data analysis/interpretation, all authors; manuscript drafting or manuscript revision for important intellectual content, all authors; manuscript final version approval, all authors; literature research, R.S.A., S.F., J.R.R., W.K., N.N.V., A.P., S.L.; clinical studies, all authors; statistical analysis, J.R.R., S.L.; and manuscript editing, R.S.A., S.F., J.R.R., A.P., S.L., R.F.W.

Authors stated no financial relationship to disclose.

References

1. Bridges-Webb C, Britt H, Miles DA, Neary S, Charles J, Traynor V. Morbidity and treatment in general practice in Australia. Aust Fam Physician 1993;22(3):336–346.[Medline]
2. Yamaguchi K, Tetro AM, Blam O, Evanoff BA, Teefey SA, Middleton WD. Natural history of asymptomatic rotator cuff tears: a longitudinal analysis of asymptomatic tears detected sonographically. J Shoulder Elbow Surg 2001;10(3):199–203.[Medline]

3. DePalma AF, White JB, Callery G. Degenerative lesions of the shoulder joint at various age groups which are compatible with good function. Instr Course Lect 1950;7:168–180.[Medline]
4. Miniaci A, Dowdy PA, Willits KR, Vellet AD. Magnetic resonance imaging evaluation of the rotator cuff tendons in the asymptomatic shoulder. Am J Sports Med 1995;23(2):142–145.[Abstract/Free Full Text]
5. Sher JS, Uribe JW, Posada A, Murphy BJ, Zlatkin MB. Abnormal findings on magnetic resonance images of asymptomatic shoulders. J Bone Joint Surg Am 1995;77(1):10–15.[Abstract/Free Full Text]
6. Tempelhof S. Rupp S, Seil R. Age-related prevalence of rotator cuff tears in asymptomatic shoulders. J Shoulder Elbow Surg 1999;8(4):296–299.
7. Rothman RH, Parke WW. The vascular anatomy of the rotator cuff. Clin Orthop Relat Res 1965;41:176–186.[Medline]
8. Rathbun JB, Macnab I. The microvascular pattern of the rotator cuff. J Bone Joint Surg Br 1970;52(3):540–553.[Medline]
9. Brooks CH, Revell WJ, Heatley FW. A quantitative histological study of the vascularity of the rotator cuff tendon. J Bone Joint Surg Br 1992;74(1):151–153.[Medline]
10. Lohr JF, Uhthoff HK. The microvascular pattern of the supraspinatus tendon. Clin Orthop Relat Res 1990;254:35–38. [Medline]
11. Biberthaler P, Wiedemann E, Nerlich A, et al. Microcirculation associated with degenerative rotator cuff lesions: in vivo assessment with orthogonal polarization spectral imaging. J Bone Joint Surg Am 2003;85-A:(3):475–480.
12. Teefey SA, Rubin DA, Middleton WD, Hildebolt CF, Leibold RA, Yamaguchi K. Detection and quantification of rotator cuff tears: comparison of ultrasonographic, magnetic resonance imaging, and arthroscopic findings in seventy-one consecutive cases. J Bone Joint Surg Am 2004;86-A:(4):708–716.
13. Seibold CJ, Mallisee TA, Erickson SJ, Boynton MD, Raasch WG, Timins ME. Rotator cuff: evaluation with US and MR imaging. RadioGraphics 1999;19(3):685–705.[Abstract/Free Full Text]
14. Averkious M, Powers J, Skyba D, Bruce M, Jenson S. Ultrasound contrast imaging research. Ultrasound Q 2003;19(1):27–37.[Medline]
15. Kitzman DW, Goldman ME, Gillam LD, Cohen JL, Aurigemma GP, Gottdiener JS. Efficacy and safety of the novel ultrasound contrast agent perfluten (Definity) in patients with suboptimal baseline left ventricular echocardiographic images. Am J Cardiol 2000;86(6):669–674.[Medline]
16. Fleischer AC, Donnelly EF, Grippo RJ, Black AS, Hallahan DE. Quantification of tumor vascularity with contrast enhanced sonography: correlation with magnetic resonance imaging and fluorodeoxyglucose autoradiography in implanted tumor. J Ultrasound Med 2004;23(1):37–41.[Abstract/Free Full Text]
17. Zanetti M, Metzdorf A, Kundert HP, et al. Achilles tendons: clinical relevance of neovascularization diagnosed with power Doppler US. Radiology 2003;227(2):556–560.[Abstract/Free Full Text]
18. Reiter M, Ulreich N, Dirisamer A, Tscholakoff D, Bucek RA. Colour and power Doppler sonography in symptomatic Achilles tendon disease. Int J Sports Med 2004;25(4):301–305.[Medline]
19. Halpern EJ, Frauscher F, Rosenberg M, Gomella LG. Directed biopsy during contrast-enhanced sonography of the prostate. AJR Am J Roentgenol 2002;178(4):915–919.[Abstract/Free Full Text]
20. Wilson SR, Burns PN. Microbubble contrast for radiological imaging. II. Applications. Ultrasound Q 2006;22(1):15–18.
21. Schueller-Weidekamm C, Krestan C, Schueller G, Kapral T, Aletaha D, Kainberger F. Power Doppler sonography and pulse-inversion harmonic imaging in evaluation of rheumatoid arthritis synovitis. AJR Am J Roentgenol 2007;188(2):504–508.[Abstract/Free Full Text]
22. Main ML, Goldman JH, Grayburn PA. Thinking outside the "box": the ultrasound. J Am Coll Cardiol 2007;50(25):2434–2437.[Abstract/Free Full Text]
23. Molloy TJ, Kemp MW, Wang Y, Murrell GA. Microarray analysis of the tendinopathic rat supraspinatus tendon: glutamate signaling and its potential role in tendon degeneration. J Appl Physiol 2006;101(6):1702–1709.[Abstract/Free Full Text]
24. Perry SM, McIlhenny SE, Hoffman MC, Soslowsky LJ. Inflammatory and angiogenic mRNA levels are altered in a supraspinatus tendon overuse animal model. J Shoulder Elbow Surg 2005;14(1 Suppl S):79S–83S.[Medline]
25. Lin TW, Cardenas L, Soslowsky LJ. Biomechanics of tendon injury and repair. J Biomech 2004;37(6):865–877.[Medline]
26. Gimbel JA, Van Kleunen JP, Mehta S, Perry SM, Williams GR, Soslowsky LJ. Supraspinatus tendon organizational and mechanical properties in a chronic rotator cuff tear animal model. J Biomech 2004;37(5):739–749.[Medline]
27. Mehta S, Gimbel JA, Soslowsky LJ. Etiologic and pathogenetic factors for rotator cuff tendinopathy. Clin Sports Med 2003;22(4):791–812.[Medline]
28. Soslowsky LJ, Thomopoulos S, Esmail A, et al. Rotator cuff tendinosis in an animal model: role of extrinsic and overuse factors. Ann Biomed Eng 2002;30(8):1057–1063.[Medline]

This Article

- Abstract FREE
- Figures Only
- AVI Movies
- Submit a response
- Alert me when this article is cited
- Alert me when eLetters are posted
- Alert me if a correction is posted

Services

- Email this article to a friend
- Similar articles in this journal
- Similar articles in PubMed
- Alert me to new issues of the journal
- Download to citation manager
- Get Permissions

Google Scholar

- Articles by Adler, R. S.
- Articles by Warren, R. F.

PubMed

- PubMed Citation
- Articles by Adler, R. S.
- Articles by Warren, R. F.

HOME | HELP | FEEDBACK | SUBSCRIPTIONS | ARCHIVE | SEARCH

RADIOLOGY | RADIOGRAPHICS | RSNA JOURNALS ONLINE